ANTICANCER RESEARCH *38*: 3435-3445 (2018)
doi:10.21873/anticanres.12612

In Vitro and *In Vivo* Antitumor Effects of Pyrimethamine on Non-small Cell Lung Cancers

MENG-XIAN LIN[1], SHENG-HAO LIN[1,2], CHI-CHEN LIN[1], CHING-CHIEH YANG[3,4,5] and SHEAU-YUN YUAN[6,7]

[1]*Institute of Biomedical Science, National Chung Hsing University, Taichung, Taiwan, R.O.C.;*
[2]*Department of Internal Medicine, Division of Chest Medicine, Changhua Christian Hospital, Changhua, Taiwan, R.O.C.;*
[3]*Department of Radiation Oncology, Chi Mei Medical Center, Tainan, Taiwan, R.O.C.;*
[4]*Institute of Biomedical Sciences, National Sun Yat-sen University, Kaohsiung, Taiwan, R.O.C.;*
[5]*Department of Pharmacy, Chia Nan University of Pharmacy and Science, Tainan, Taiwan, R.O.C.;*
[6]*Department of Medical Research, Taichung Veterans General Hospital, Taichung, Taiwan, R.O.C.;*
[7]*Department of Nursing, Hungkuang University, Taichung, Taiwan, R.O.C.*

Abstract. *Background/Aim: Pyrimethamine (PYR), an anti-malarial drug is known to inhibit various types of human cancer cells. The aim of this study was to investigate the anti-tumour effects of pyrimethamine (PYR) and its underlying molecular mechanisms using the human NSCLC cell line A549. Materials and Methods: PYR was dissolved in dimethyl sulfoxide to determine its apoptotic activity on A549 cells. Cell viability was determined by the MTT assay. Cell cycle, mitochondrial membrane potential, and Annexin V-FITC early apoptosis detection were evaluated by flow cytometry. Cyclin-dependent kinase (CDK) and Bcl-2 family protein expression was determined by western blotting. Results: PYR reduced cell viability percentage and induced G_0/G_1 arrest, which was associated with down-regulation of cyclins D1 and E, CDK4, and CDK2, and up-regulation of p21. PYR induced sub-G_1 accumulation, Annexin-V binding, caspase-9 and -3 activation, poly (ADPribose) polymerase cleavage, and mitochondrial dysfunction in A549 cells. Moreover, PYR effectively inhibited NSCLC tumour growth in an A549 xenograft model. Conclusion: PYR demonstrated anti-tumour effects on NSCLC in vitro and in vivo, indicating its therapeutic potential against human NSCLC.*

Correspondence to: Dr. Sheau-Yun Yuan, Department of Medical Research, Taichung Veterans General Hospital, No. 1650 Section 4, Boulevard, Situn, Taichung 40705, Taiwan, R.O.C. Tel: +886 423592525#4019, Fax: +886 423592705, e-mail: yuan5805@gmail.com or Dr. Ching-Chieh Yang, Department of Radiation Oncology, Chi-Mei Medical Center, No. 901, Zhonghua Road,Tainan 71004, Taiwan, R.O.C. Tel: +886 62812811#53501, Fax: +886 62820049, e-mail: cleanclear0905@gmail.com

Key Words: Non-small cell lung cancer (NSCLC), pyrimethamine, cell cycle, apoptosis, mitochondrial damage.

The incidence of lung cancer continues to rise and has become the leading cause of cancer deaths worldwide (1). Two major types, non-small cell lung cancers (NSCLCs) and small-cell lung cancers (SCLCs) can be identified. NSCLCs account for approximately 80% of all cases. Surgery is regarded the primary treatment modality for NSCLCs, but only 20-25% of the tumors are suitable for potentially curative resection. As a result, more effective treatments, such as chemotherapy (CT) or chemotherapy concurrent with radiotherapy (RT) to improve recurrence and mortality rates, are needed (2). Different chemotherapeutic agents have been used for NSCLCs to improve prognosis. However, NSCLCs are relatively resistant to chemotherapy, and the 5-year survival rate is as low as 20% (3). Therefore, there is an urgent need to identify or develop new agents to improve sensitivity or resistance to current chemotherapy in the treatment of NSCLC.

Despite intensive research, improvements in the treatment of NSCLCs have remained deficient. Currently, the chemotherapy use for NSCLCs often consists of a combination of drugs, the most commonly used being cisplatin-based plus docetaxel (Taxotere), gemcitabine (Gemzar), paclitaxel (Taxol and others), vinorelbine (Navelbine and others) and so on (4). These cytotoxic drugs, irrespective of their intracellular target, have been shown to cause cell death in sensitive cells, at least partly, by inducing apoptosis. Apoptosis, a process of programmed cell death, could be induced by activation of caspases in the extrinsic pathway or through mitochondrial damage and apoptotic protein activation in the intrinsic pathway. Therefore, different biochemical targets or agents that play a role in intrinsic and extrinsic apoptotic pathways should be investigated for cancer treatment (5-8).

Pyrimethamine (PYR), a folic acid antagonist, can indirectly block the synthesis of nucleic acids by inhibiting the enzyme dihydrofolate reductase (DHFR) (9). Currently, it is effectively used in the prevention and treatment of opportunistic infections such as malaria and toxoplasmosis (10, 11). Several investigators have noted that PYR has antitumor activity. Giammarioli *et al*. indicated that PYR induced apoptosis through caspase and cathepsin mechanisms in melanoma cells (12). PYR is also reported to enhance temozolomide-induced cytotoxicity in melanoma cells and invasive pituitary adenomas (13, 14). Moreover, PYR is known to sensitize temozolomide-resistant glioblastoma and act as a selective inhibitor in acute myeloid leukemia (15, 16). Furthermore, PYR also suppressed the telomerase activity in the PC-3 prostate cancer cell line (17) and inhibited the matrix metalloproteinases (MMP) type 2 activity in fibrosarcoma (18). However, no data on the role of PYR in NSCLC cells are presently available or extensively studied.

Therefore, in this study, the *in vitro* and *in vivo* antitumor activity of PYR was studied in the human NSCLC cell line A549. In addition, the possible molecular mechanisms responsible for its anticancer activity were also investigated.

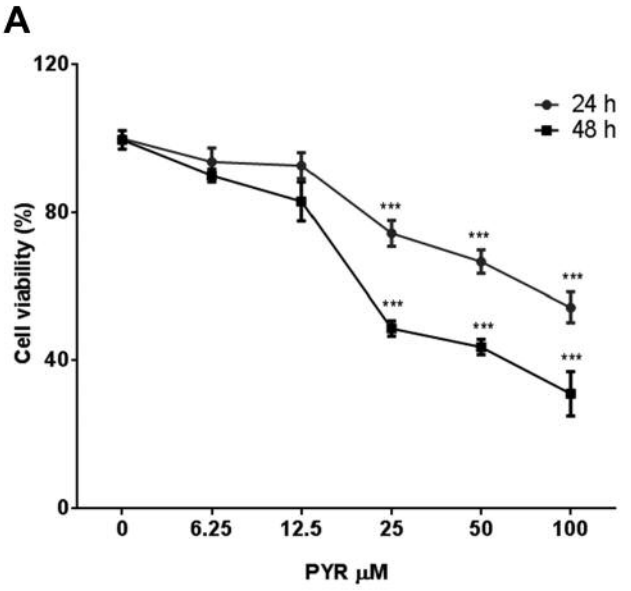

Figure 1. *Continued*

Materials and Methods

Cell lines and culture conditions. The NSCLC cell line A549 was purchased from the American Type Culture Collection (ATCC®) (Manassas, VA, USA). The human NSCLC cell line A549 was maintained in RPMI with 10% fetal bovine serum, 1% penicillin and streptomycin (Gibco/BRL, Gran Island, NY, USA) and was cultured at 5% CO_2 and saturated humidity at 37˚C in an incubator.

Cell viability assay. The A549 cells were seeded at 1×10^4 in a 24-well dish overnight. Pyrimethamine (Sigma-Aldrich, St. Louis, MO, USA) was dissolved in dimethyl sulfoxide (DMSO; Sigma-Aldrich) at 100 mM as stock solution for *in vitro* assays. The cells were treated with 25, 50 and 100 μM for 24 h, 48 h and 72 h. Then, the cells were cultured with 1 mg/ml 3-(4,5-Cimethylthiazol-2-yl)-2,5-diphenyl tetrazolium bromide (MTT) (BioVision, Milpitas, CA, USA) for 4 h, after which the medium was removed. The wells were washed once with Phosphate-buffered saline (PBS), and formazan was dissolved in DMSO. The solution was measured by microplate reader (Tecan Sunrise, San Jose, CA, USA) at 540 nm.

Cell-cycle assay. The A549 cells were seeded at 1×10^5 in a 6-well dish overnight. The cells were treated with 25, 50 and 100 μM pyrimethamine for 24, 48 and 72 h. The cells were collected and washed with PBS, and then, the cells were fixed in 70% ethanol and kept at –20˚C for 16 h or overnight. The cells were washed with PBS and stained with propidium iodide (PI) solution (containing 2 mg/ml RNase, 1 mg/ml PI and 5% Triton X-100) (Sigma-Aldrich) for 30 min at RT and kept away from light. Fluorescence intensity in all samples was detected and measured using an Accuri™ C5 cytometer (BD Biosciences, San Jose, CA, USA).

Annexin V-FITC/PI staining assay. The A549 cells were seeded at 1×10^5 in a 6-well dish overnight. The cells were treated with 25, 50 and 100 μM pyrimethamine for 24, 48 and 72 h. The cells were collected and washed with PBS and stained with Annexin-V/PI solution (containing 2 μl Annexin V, 2 μl PI and 100 μl binding buffer) (BioVision, Milpitas, CA, USA) for 15 min at RT and kept away from light. The fluorescence intensity of all samples was detected and measured using an Accuri™ C5 cytometer (BD Biosciences).

Caspase-3, 8, and 9 activities Assay. After treatment with PYR for 48 h, cells were harvested for examination of caspase-3, 8, and 9 activities using the appropriate CaspGLOW™ Fluorescein Active Caspase Staining Kits (Biovision, Milpitas, CA, USA) according to the manufacturer's specifications.

Mitochondrial membrane potential detection. The A549 cells were seeded at 1×10^5 in a 6-well dish overnight. The cells were treated with 25, 50 and 100 μM pyrimethamine for 24, 48 and 72 h. The cells were collected, washed with PBS and stained with 10 μg/ml JC-1 (Life Invitrogen, Carlsbad, CA, USA) for 10 min at RT and kept away from light. The fluorescence intensity of all samples was detected and measured using an Accuri™ C5 cytometer (BD Biosciences).

Cytochrome c level assay. The A549 cells were seeded at 1×10^5 in a 6-well dish overnight. The cells were treated with 25, 50 and 100 μM pyrimethamine for 24 h, 48 h and 72 h. Cells were then collected, washed with PBS and the cell membrane was permeabilized with 1 mg/ml digitonin buffer for 5 min in ice and washed with PBS containing 0.1% BSA. The samples were fixed and processed with a Cytofix/Cytoperm Plus Kit (BD Biosciences) according to the manufacturer's instructions. Next, the samples were incubated with cytochrome *c*-FITC antibody for 1 h in ice and kept away from light. The fluorescence intensity of all samples was detected and measured using an Accuri™ C5 cytometer (BD Biosciences).

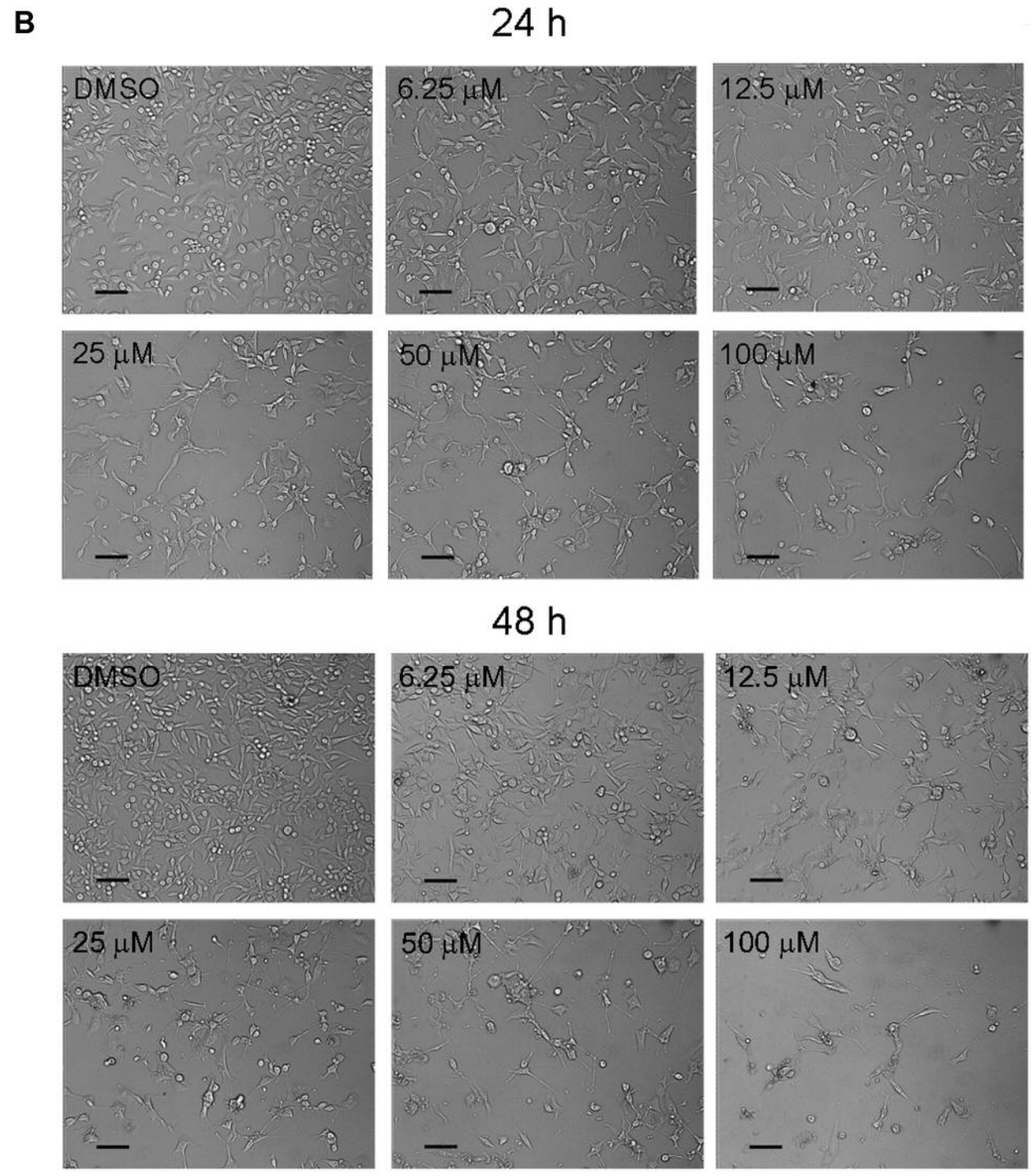

Figure 1. *Continued*

Western blotting. The A549 cells were seeded at 1×10^6 in a 10-cm dish overnight. The cells were treated with 25, 50 and 100 μM pyrimethamine for 24 h and collected to analyze the level of cell cycle-associated protein and apoptotic-related protein. The cells were lysed in RIPA lysis buffer containing protease inhibitor and phosphatase inhibitor, and protein concentration was measured using a BCA protein assay kit (Thermo Fisher Scientific, Waltham, MA, USA). Thirty micrograms of proteins were separated by SDS-polyacrylamide gel electrophoresis and transferred to a PVDF membrane. The membrane was incubated with primary antibody at

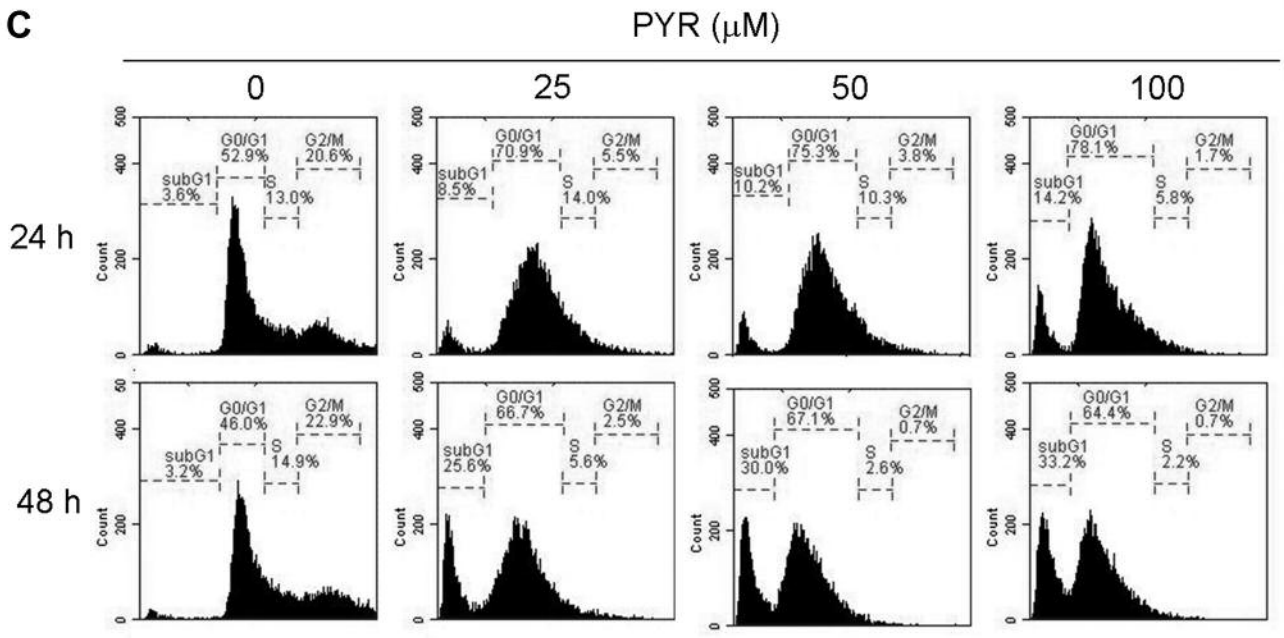

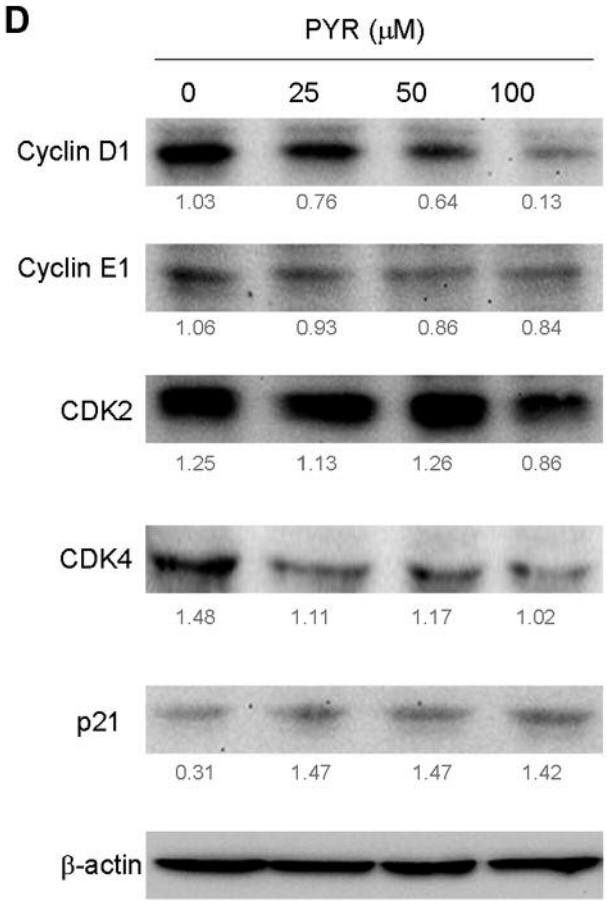

Figure 1. *Cell viability and cell-cycle distribution of A549 cells with PYR treatments. A: Cell viability was examined by MTT assay. Data are expressed as a percentage of the control treated with DMSO. Each point on the graph represents means±SD from triplicate tests for each treatment. ***p<0.001 compared with DMSO-treated control. B: The morphology of A549 cells treated with different dosages of PYR for 24 h and 48 h were examined under phase-contrast microscopy and photographed (400×). C: Detection of cell cycle distributions after PYR treatment by propidium iodide (PI) staining and subsequent flow cytometric analysis. D: A549 cells were treated with different dosages of PYR for 24 h, and western blotting was used to evaluate the expression levels of cell cycle regulatory proteins. β-actin expression was measured as an internal control for equal protein loading. All experiments were repeated more than three times with similar results.*

4˚C overnight. After that, the membrane was incubated with peroxidase-labeled secondary antibody for 4˚C overnight. The immunofluorescence signals were detected with an enhanced chemiluminescence (ECL) system and developed using the LAS3000 system (Fujifilm, Valhalla, NY, USA). Densitometric analysis performed in this study was conducted using Image J software (National Institute of Health, Bethesda, MD, USA). In this study, the primary antibodies were anti-BCL-xL (1:1,000 dilution; clone S-18, CAS:sc-634, Santa Cruz, St. Louis, MO, USA), anti-Bak (1:1,000 dilution;, CAS:sc-832, Santa Cruz), anti-BCL-2 (1:1,000 dilution; clone 50E3, CAS:2870, Cell Signaling, Beverly, MA, USA), anti-CDK2 (1:5,000 dilution; clone E304, catalog:1134-5, Epitomics, Cambridge, MA, USA), anti-CDK4 (1:1,000 dilution; clone polyclonal, catalog:S1572, Epitomics), anti-Cyclin D1 (1:1,0000 dilution; clone EPR2241(IHC)-32, catalog:2261-5, Epitomics), anti-Cyclin E (1:1,000 dilution; clone D7T3U, CAS:20808, Cell Signaling), anti-p21 (1:10,000 dilution; clone EP1125Y, catalog:ab52939, Abcam, Cambridge, MA, USA), and anti-β-actin (1:1,000;clone C4, CAS:sc-47778, Santa Cruz). The blots were quantified by densitometric analysis using Image J software version 1.47 (National Institutes of Health, Bethesda, MD, USA).

Animal. Female BALB/c *nu/nu* mice (n=24; 4-weeks-old; 20-25 g) were purchased from the National Laboratory Animal Center (Taipei, Taiwan). The mice were housed in cages with free access to food and water at controlled temperature (22±2˚C) and humidity (45-65%) on a 12-h light/dark cycle. All animal procedures were conducted according to institutional guidelines and approved by the Institutional Animal Care and Utilization Committee of National Chung Hsing University, Taiwan (approval protocol no. NCHU-IACUC NO. 105-104).

Xenograft animal model. Quantities of 1×10^7 A549 cells were injected into the right flanks of 6-week-old female BALB/c *nu/nu* mice. When the tumors were established (day 10), the mice were randomly divided into two groups: the vehicle control group was given 10% DMSO + 90% glyceryl trioctanoate (Sigma-Aldrich), while the PYR treatment group received 30 mg/kg of PYR *via* intraperitoneal injection (*i.p.*) once a day. The tumor volume was measured once every five days. On day 35, mice were sacrificed by gradual-fill 100% CO_2 inhalation (rate of 30-40% of the chamber volume per minute) and tumors were extracted, photographed and weighed. The tumor volume was measured by the following formula, length × width × width/2, and averaged (mean±standard error of mean).

Statistical analyses. Statistical analyses and graphics were performed using GraphPad Prism Version 5.0 (San Diego, CA, USA). The Mann–Whitney *U*-test was used to compare the two groups based on the animal experiments. For comparison between the control and drug-treatment groups, the two-tailed *t*-test (Student's *t*-test) was used. A *p*-value less than 0.05 was considered statistically significant.

Results

PYR inhibits cell proliferation through G_1 phase arrest. First, we evaluated the dose-dependent and time-dependent effect of PYR on the NSCLC A549 cell line. As shown in Figure 1A, PYR can gradually reduce the cell viability of A549 with higher concentrations and longer times. In addition, microscopic examination revealed that morphological changes in cell shape such as shrinkage, rounding, and floating of the cells were observed with increasing concentrations of PYR (Figure 1B). To further assess the effect of PYR on cell proliferation, we tested the fluorescence intensity by flow cytometry during different cell cycles. For the A549 cell line, PYR induced G_1 and sub-G_1 phase accumulation of cells after 24 h treatment, as shown in Figure 1C. In addition, the number of cells at the sub-G_1 phase increased at different PYR concentrations (25, 50, 100 μM) (Figure 1C) at 48 h. The western blotting results also showed that incubation with PYR for 24 h reduced the expression of G_1 phase-related proteins, including CDK4, CDK2, cyclin E and cyclin D1; however, the expression of Cdk2 inhibitor $p21^{Cip1}$ was increased (Figure 1D). These results suggest that PYR can inhibit cell proliferation *via* G_1 phase arrest.

PYR promotes apoptosis by inducing apoptotic protein activation. Next, the effect of PYR on apoptosis of A549 cells was investigated. Previous literature has reported that apoptotic cells express phosphatidylserine (PS) on the surface (19, 20). In this study, PYR stimulated PS expression, as shown by flow cytometry using Annexin V-FITC staining. As depicted in Figure 2A, PYR dose-dependently induced PS expression after 48 h. The results of the caspase activity assay also revealed that PYR significantly increased caspase-9 and caspase-3 activities at 48 h but not caspase-8 activity (Figure 2B). In addition, western blotting results showed that the mitochondrial membrane pro-apoptotic protein Bak was increased and anti-apoptotic proteins Bcl-xL and BCl-2 were decreased (Figure 2C). The alteration of Bak and Bcl-2 levels resulted in an increase in the ratio of Bak to Bcl-2 (Figure 2D). Furthermore, PYR induced sub-G_1 phase accumulation at 48 h, as shown in Figure 1B. These results indicated that PYR inhibits cell proliferation *via* activation of apoptosis.

PYR induces apoptosis via mitochondrial dysfunction and cytochrome c release. Due to the increased Bak and decreased BCl-2 and Bcl-xL levels found in western blotting, as well as the cleavaged-caspase-8 not activated by PYR, it is evident that PYR may cause cancer cell apoptosis *via* the mitochondrial (intrinsic) apoptotic pathway. Mitochondrial membrane potential (MMP) analysis revealed that JC-1, an indicator for MMP, forms monomers (green fluorescence) in low-MMP conditions and JC1-aggregates (red fluorescence) in normal conditions. As shown in Figure 3A, PYR can reduce the mitochondrial membrane potential by inducing green fluorescence accumulation at 48 h. This reduced mitochondrial membrane potential also enhances the cytochrome *c* release into the cytosol, as shown in Figure 3B. These results suggest that PYR can induce apoptosis *via* mitochondrial dysfunction.

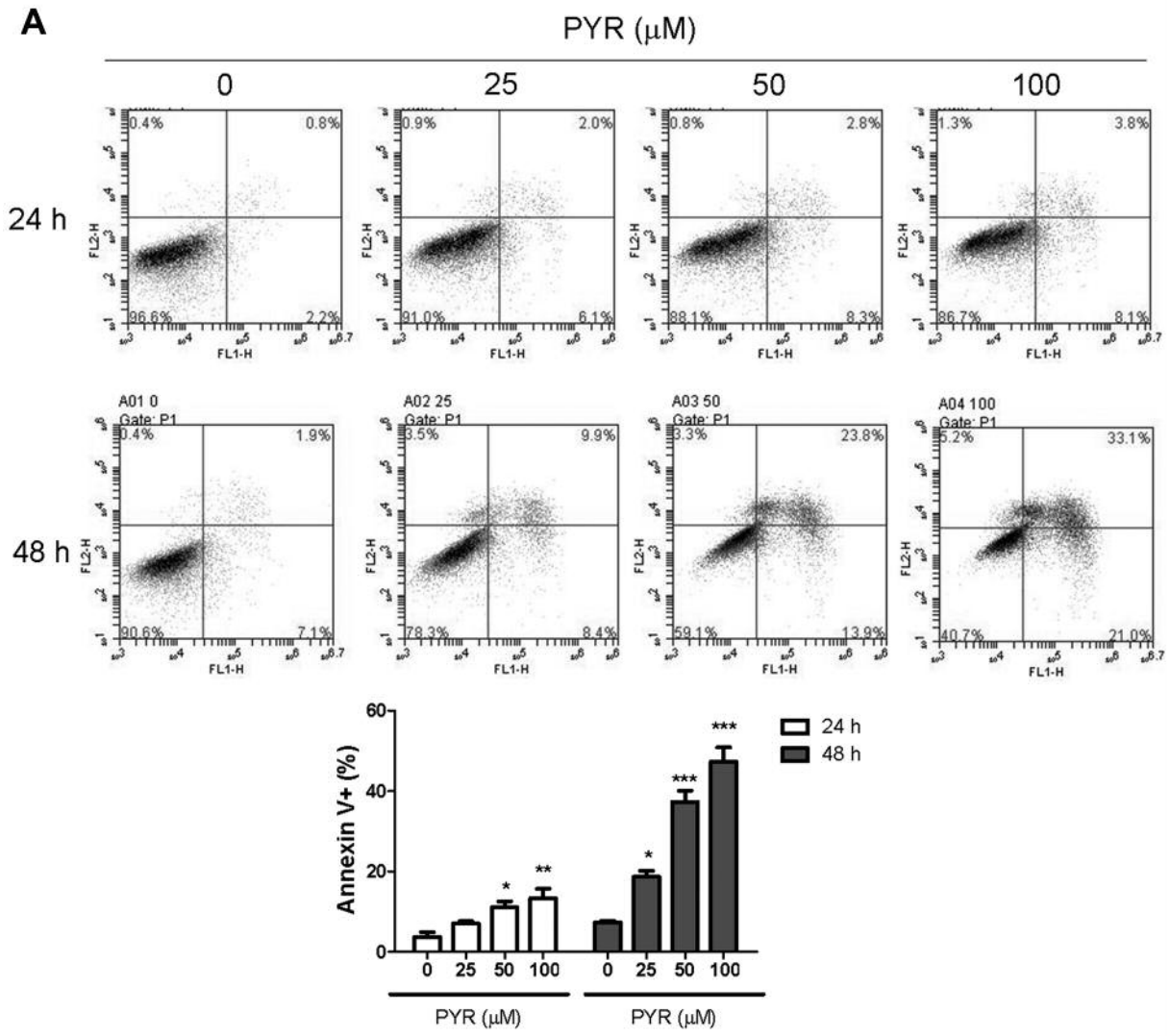

Figure 2. *Continued*

PYR suppresses tumor growth in xenograft animal model. In a xenograft animal model, it was observed that PYR inhibited tumor growth in tumor-bearing mice. On day 10, the PYR (30 mg/kg)-injected mice group revealed a reduction in tumor growth, as shown in Figure 4A. After these mice were sacrificed on day 35, the PYR-treated tumor size was significantly smaller, and the average weight was also lighter than the vehicle control group (Figure 4B-C). These results supported that PYR could suppress tumor growth *in vivo*.

Discussion

This is the first study to determine the *in vitro* and *in vivo* antitumor activity of PYR in human NSCLC cells. In the present work, our data showed that PYR promotes the death of cancer cells through G_1 cell-cycle arrest and the intrinsic (mitochondrial mediated) apoptotic pathway in the NSCLC cell line. The *in vivo* antitumor effect of PYR was also observed in a severe SCID-mouse xenograft model experiment.

Lung cancer is common worldwide, with an estimated 1.56 million deaths annually (1). Patients can receive combined modality with surgery, chemotherapy and radiotherapy for advanced disease, but the outcome has remained stagnant in the past several decades (2). Recently, PYR, which is an anti-folate drug, has been studied as an antitumor agent or chemotherapy enhancer (13, 17). However, its antitumor effect for lung cancer is so far unknown. Previous reports have indicated that PYR could induce apoptosis and S-phase accumulation in many cancer cell lines (12, 21, 22). However, in this study PYR induced the G_0/G_1 phase arrest and

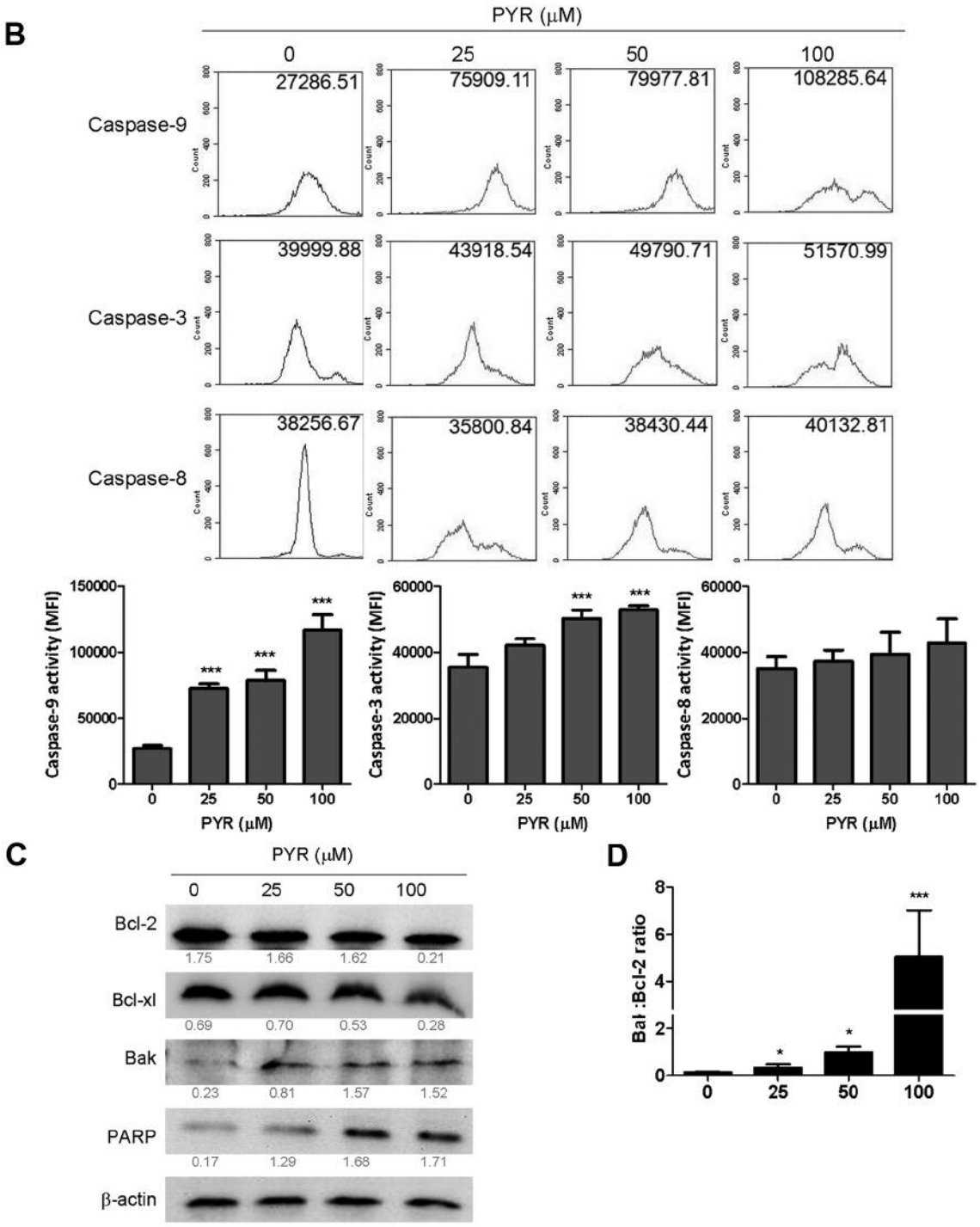

Figure 2. *Analysis of PYR-induced apoptosis in A549 cells. A: A549 cells were treated with different dosages of PYR for 24 and 48 h. Phosphatidylserine externalization and DNA integrity were analyzed by Annexin-V-FITC and PI staining, respectively. The lower-right quadrant (annexin-V$^+$/PI$^-$) is considered early-stage apoptotic cells, while the upper-right quadrant (annexin V$^+$/PI$^+$) indicates late apoptotic cells. The bar graph at the bottom represents the means±SD of the experimental triplicates. *p<0.05, **p<0.01, ***p<0.001 compared with control. B: A549 cells were treated with PYR or DMSO for 48 h, and then, the activities of caspase-3, -8, and -9 were determined by flow cytometry. ***p<0.001 compared with control. C: A549 cells were treated with different dosages of PYR for 48 h, and western blotting was used to evaluate the expression levels of Bcl-2, Bcl-xL and Bax proteins. β-actin expressions were measured as an internal control for equal protein loading. All experiments were repeated more than three times with similar results. D: After normalization with the intensity of β-actin using an image J analysis program, the ratio of Bcl-2 to Bak protein was determined. *p<0.05, ***p<0.001 compared to control.*

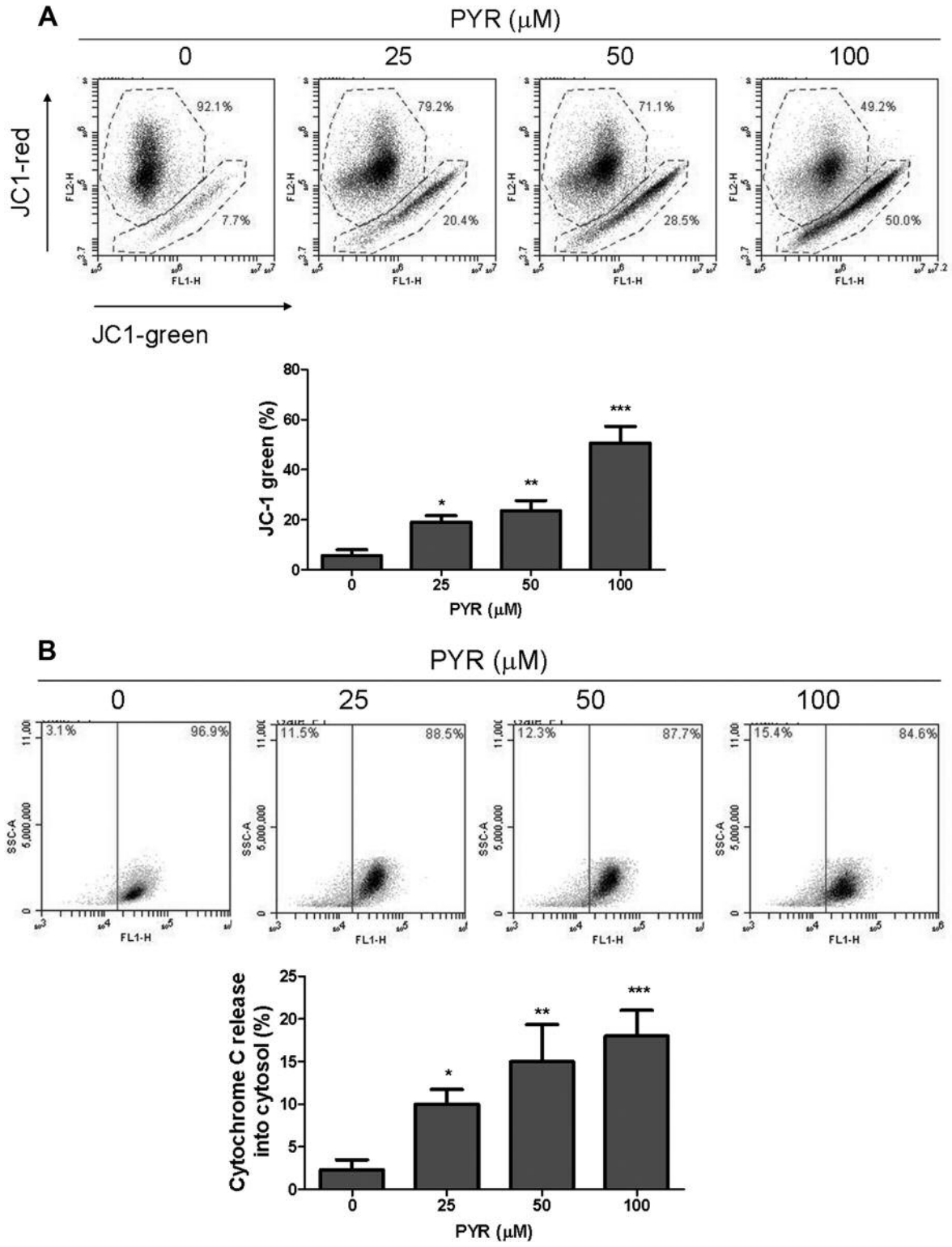

Figure 3. *PYR induced MMP reduction and cytochrome c release in A549 cells. A549 cells were treated with different dosages of PYR for 48 h. A: Mitochondrial membrane potential (Δψm) was analyzed by JC-1 staining and assessed by flow cytometry. The bar graph at the bottom represents the means±SD of the experimental triplicates. B: Cytochrome c expression in cytosol was determined by anti-cytochrome c-FITC staining and flow cytometry analysis. All experiments were repeated more than three times with similar results. Significant differences compared to the DMSO-treated control group are indicated by **p<0.01, **p<0.01, ***p<0.001.*

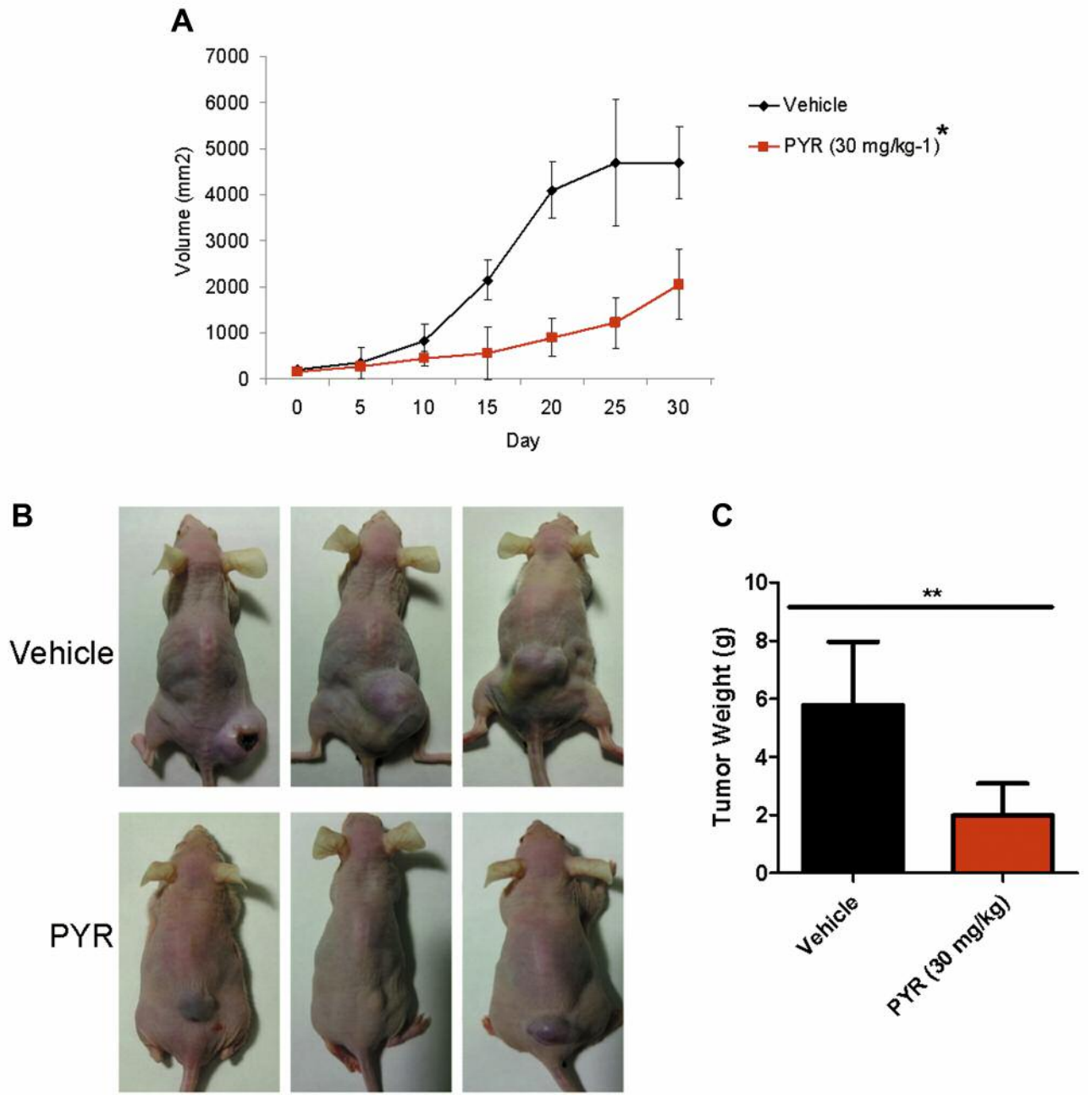

Figure 4. *PYR inhibited A549 tumor growth in nude mice. A549 cells (1×10^7) were subcutaneously injected into mice, producing a visible tumor (approximately 10 mm^3). PYR (30 mg/kg) and vehicle control were administered intraperitoneally 3 times/week until day 35 (n=6). (A) The graph shows the tumor volume changes with time. (B) Tumor tissue was photographed (C) and the tumor weight at day 35 was examined. Both quantified data are presented as the means±SD. *p<0.05, **p<0.01 denotes the comparisons between PYR and vehicle groups.*

increased sub-G_1 phase accumulation. The results of western blotting also showed that the levels of cyclin E, cyclin D1, CDK4 and CDK2 were reduced, but p21 was increased. These results suggested that PYR inhibits NSCLC proliferation by incomplete DNA synthesis and cell division.

Although cell death can occur through non-apoptotic mechanisms, apoptosis is the major mechanism of action of chemotherapeutic agents against cancer cells (23, 24). Thus, induction of apoptosis is considered to be a potent therapeutic strategy in the eradication of tumors, especially

lung malignance (25, 26). To test this, we analyzed the activity of caspases 3, 8, and 9. Caspase-3 is the most important component of the apoptotic pathway and can be activated by caspase-8 or -9, the two key proteins of the extrinsic and intrinsic apoptotic pathways, respectively. The mechanism underlying PYR-induced apoptosis has been investigated for years. Dai *et al*. reported that PYR caused a significant increase in the activities of caspase 3/7, 8, 9 in melanoma cell lines (14). Consistent with another previous report (12), the apoptotic proteins caspase-9 and -3, but not caspase-8, were activated in our study, indicating that PYR exerts its effects *via* the intrinsic apoptotic pathway.

Because PYR induced apoptosis through the intrinsic pathway (mitochondrial damage), we further attempted to analyze the related pathway. If the mitochondria were damaged, the mitochondria membrane potential (MMP) would be decreased at the same time. In mitochondrial membrane potential (MMP) analysis, JC-1, an indicator for MMP, showed a reduced expression of green fluorescence accumulation. Also, flow cytometry analysis of cytochrome *c*-FITC staining indicated that PYR induced mitochondria to release cytochrome c into the cytoplasm. Apoptosis regulator Bcl-2 family proteins, either pro-apoptotic (such as Bax, BAD, Bak) or anti-apoptotic (Bcl-2 proper, Bcl-xL), are the two major types that regulate mitochondria-related apoptosis (27). In our results, the levels of Bcl-2 and Bcl-xL were reduced, but Bak was significantly increased at 48 h (Figure 2C). These results suggest that PYR induces apoptosis through the mitochondria-damaged pathway.

In conclusion, the results of the present study showed that PYR promoted the death of cancer cells through G_1 cell-cycle arrest and the intrinsic (mitochondrial mediated) apoptotic pathway in the NSCLC cell line. Inhibition of cell proliferation suggests that PYR could be used for anti-cancer therapy. Further study is needed to evaluate its efficacy when combined with current chemotherapy regimens.

Conflicts of Interest

The Authors have no conflict of interest associated with the manuscript.

Acknowledgements

The Authors thank the reviewers for their helpful comments on this article and the present study was supported by Changhua Christian Hospital (grant nos. 103-CCH-IRP-003 and 103-CCH-ICO-001).

References

1 Siegel R, Ma J, Zou Z and Jemal A: Cancer statistics, 2014. CA Cancer J Clin *64(1)*: 9-29, 2014.

2 Lemjabbar-Alaoui H, Hassan OU, Yang YW and Buchanan P: Lung cancer: Biology and treatment options. Biochim Biophys Acta *1856(2)*: 189-210, 2015.

3 Cronin KA, Ries LA and Edwards BK: The surveillance, epidemiology, and end results (seer) program of the national cancer institute. Cancer *120(Suppl 23)*: 3755-3757, 2014.

4 Ettinger DS and Kris MG: Update: Nccn non-small cell lung cancer clinical practice guidelines. J Natl Compr Canc Netw *2(Suppl 3)*: S-9-13, 2004.

5 Li C, Chen S, Yue P, Deng X, Lonial S, Khuri FR and Sun SY: Proteasome inhibitor ps-341 (bortezomib) induces calpain-dependent ikappab(alpha) degradation. J Biol Chem *285(21)*: 16096-16104, 2010.

6 Park MT, Kang JA, Choi JA, Kang CM, Kim TH, Bae S, Kang S, Kim S, Choi WI, Cho CK, Chung HY, Lee YS and Lee SJ: Phytosphingosine induces apoptotic cell death *via* caspase 8 activation and bax translocation in human cancer cells. Clin Cancer Res *9(2)*: 878-885, 2003.

7 Tsai JJ, Hsu FT, Pan PJ, Chen CW and Kuo YC: Amentoflavone enhances the therapeutic efficacy of sorafenib by inhibiting anti-apoptotic potential and potentiating apoptosis in hepatocellular carcinoma *in vivo*. Anticancer Res *38(4)*: 2119-2125, 2018.

8 Kim MJ, Kwon SB, Kim MS, Jin SW, Ryu HW, Oh SR and Yoon DY: Trifolin induces apoptosis *via* extrinsic and intrinsic pathways in the nci-h460 human non-small cell lung-cancer cell line. Phytomedicine *23(10)*: 998-1004, 2016.

9 Olliaro PL and Yuthavong Y: An overview of chemotherapeutic targets for antimalarial drug discovery. Pharmacol Ther *81(2)*: 91-110, 1999.

10 Wilson T and Edeson JF: Treatment of acute malaria with pyrimethamine. Br Med J *1(4804)*: 253-255, 1953.

11 Gomes TC, de Andrade Junior HF, Lescano SA and Amato-Neto V: *In vitro* action of antiparasitic drugs, especially artesunate, against toxoplasma gondii. Rev Soc Bras Med Trop *45(4)*: 485-490, 2012.

12 Giammarioli AM, Maselli A, Casagrande A, Gambardella L, Gallina A, Spada M, Giovannetti A, Proietti E, Malorni W and Pierdominici M: Pyrimethamine induces apoptosis of melanoma cells *via* a caspase and cathepsin double-edged mechanism. Cancer Res *68(13)*: 5291-5300, 2008.

13 Chen M, Osman I and Orlow SJ: Antifolate activity of pyrimethamine enhances temozolomide-induced cytotoxicity in melanoma cells. Mol Cancer Res *7(5)*: 703-712, 2009.

14 Dai C, Zhang B, Liu X, Guo K, Ma S, Cai F, Yang Y, Yao Y, Feng M, Bao X, Deng K, Jiao Y, Wei Z, Junji W, Xing B, Lian W and Wang R: Pyrimethamine sensitizes pituitary adenomas cells to temozolomide through cathepsin b-dependent and caspase-dependent apoptotic pathways. Int J Cancer *133(8)*: 1982-1993, 2013.

15 Baritchii A, Jurj A, Soritau O, Tomuleasa C, Raduly L, Zanoaga O, Cernea D, Braicu C, Neagoe I and Stefan Florian I: Sensitizer drugs for the treatment of temozolomide-resistant glioblastoma. J buon *21(1)*: 199-207, 2016.

16 Sharma A, Jyotsana N, Lai CK, Chaturvedi A, Gabdoulline R, Gorlich K, Murphy C, Blanchard JE, Ganser A, Brown E, Hassell JA, Humphries RK, Morgan M and Heuser M: Pyrimethamine as a potent and selective inhibitor of acute myeloid leukemia identified by high-throughput drug screening. Curr Cancer Drug Targets *16(9)*: 818-828, 2016.

17 Khorramizadeh MR, Saadat F, Vaezzadeh F, Safavifar F, Bashiri H, Jahanshiri Z, Momeny M and Mirshafiey A: Suppression of telomerase activity by pyrimethamine: Implication to cancer. Iran Biomed J *11(4)*: 223-228, 2007.

18 Saadat F, Khorramizadeh MR and Mirshafiey A: Chemoprevention by pyrimethamine. Immunopharmacol Immunotoxicol *27(2)*: 233-240, 2005.
19 Peng L, Jiang H and Bradley C: Annexin v for flow cytometric detection of phosphatidylserine expression on lymphoma cells undergoing apoptosis. Hua Xi Yi Ke Da Xue Xue Bao *32(4)*: 602-604, 620, 2001.
20 Martin SJ, Reutelingsperger CP, McGahon AJ, Rader JA, van Schie RC, LaFace DM and Green DR: Early redistribution of plasma membrane phosphatidylserine is a general feature of apoptosis regardless of the initiating stimulus: Inhibition by overexpression of bcl-2 and abl. J Exp Med *182(5)*: 1545-1556, 1995.
21 Huang RF, Ho YH, Lin HL, Wei JS and Liu TZ: Folate deficiency induces a cell cycle-specific apoptosis in hepg2 cells. J Nutr *129(1)*: 25-31, 1999.
22 James SJ, Pogribny IP, Pogribna M, Miller BJ, Jernigan S and Melnyk S: Mechanisms of DNA damage, DNA hypomethylation, and tumor progression in the folate/methyl-deficient rat model of hepatocarcinogenesis. J Nutr *133(11 Suppl 1)*: 3740s-3747s, 2003.
23 Aleo E, Henderson CJ, Fontanini A, Solazzo B and Brancolini C: Identification of new compounds that trigger apoptosome-independent caspase activation and apoptosis. Cancer Res *66(18)*: 9235-9244, 2006.
24 Du J, Sun Y, Lu YY, Lau E, Zhao M, Zhou QM and Su SB: Berberine and evodiamine act synergistically against human breast cancer mcf-7 cells by inducing cell cycle arrest and apoptosis. Anticancer Res *37(11)*: 6141-6151, 2017.
25 Ichihara H, Kuwabara K and Matsumoto Y: Trehalose liposomes suppress the growth of tumors on human lung carcinoma-bearing mice by induction of apoptosis *in vivo*. Anticancer Res *37(11)*: 6133-6139, 2017.
26 Pinkhien T, Maiuthed A, Chamni S, Suwanborirux K, Saito N and Chanvorachote P: Bishydroquinone renieramycin m induces apoptosis of human lung cancer cells through a mitochondria-dependent pathway. Anticancer Res *36(12)*: 6327-6333, 2016.
27 Zhang H, Holzgreve W and De Geyter C: Bcl2-l-10, a novel anti-apoptotic member of the bcl-2 family, blocks apoptosis in the mitochondria death pathway but not in the death receptor pathway. Hum Mol Genet *10(21)*: 2329-2339, 2001.

Received March 27, 2018
Revised April 27, 2018
Accepted April 30, 2018